

Supporting Information for the Environmental Science and Technology Letters article:

Enhanced inactivation of *Cryptosporidium parvum* oocysts during solar photolysis of free available chlorine

Peiran Zhou,[†] George D. Di Giovanni,[§] John S. Meschke,^{†,‡} Michael C. Dodd,^{†,‡,*}

[†]Dept. of Civil and Environmental Engineering, University of Washington, Seattle, WA 98195

[‡]Dept. of Env. and Occupational Health Sciences, University of Washington, Seattle, WA 98195

[§]Univ. of Texas-Houston School of Public Health, El Paso Regional Campus, El Paso, TX 79902

Author e-mail addresses: peiran@uw.edu, george.d.digiovanni@uth.tmc.edu,
jmeschke@uw.edu, doddm@uw.edu

*Corresponding author contact details:

305 More Hall, Box 352700; Seattle, WA 98195-2700
206-685-7583; fax: 206-543-1543; e-mail: doddm@uw.edu

11 pages, including 5 narratives, 2 tables, 4 figures, 1 scheme, and supporting references

Text S1. Natural Surface Water Source and Sample Characterization

A four-liter grab sample was collected from the regulating basin of Seattle Public Utilities' Tolt River water treatment plant, where the water source is the South Fork Tolt River. At the Tolt facility, water is impounded within the South Fork Tolt Reservoir prior to conveyance through a pipeline to a regulating basin located roughly two miles from the main plant. From the regulating basin, raw water is piped into the main plant, where it is ozonated, amended with ferric chloride, filtered through anthracite coal, and finally chlorinated prior to passage into the distribution system. The water sample was stored at 4° C and filter sterilized prior to use (using a 0.2 µm Thermo Scientific Nalgene disposable filter unit), in order to remove any potential microbial contamination while minimizing alterations to the native chemical characteristics of the water. The filter was flushed with at least 1 L of the Tolt water prior to filtrate collection, in order to prevent filtrate contamination by carbon originating from the filters. Prior to use in experiments, the water sample was buffered with sterile 10-mM phosphate to pH 8. Water quality parameters for the sample are summarized in Table S1.

Text S2. HCT-8 Cell Line Maintenance and Infectious Oocyst Enumeration Procedures

HCT-8 cell line maintenance. HCT-8 cells were routinely passaged on Mondays and Thursdays. All cells used for infections were within their 30th passage. On Mondays, a flask of HCT-8 cells was set up to enable seeding of 48-well plates on Wednesdays as needed. HCT-8 seeded 48-well plates were inoculated with oocyst samples on Friday and stained for enumeration of oocyst infectivity on Mondays.

Infectious oocyst enumeration. Following staining, the numbers of infectious foci (defined as clusters of *Cryptosporidium* intracellular developmental stages originating from

infection by a single oocyst) in each sample aliquot were counted at 40× magnification, using an inverted epifluorescence microscope with MetaMorph® Microscopy Automation & Image Analysis Software to scan individual 1 mm² sections of a grid spanning the entirety of the well corresponding to that sample aliquot. An infectious focus was defined in accord with previous conventions,¹ where an individual focus was taken to comprise ≥3 visible *Cryptosporidium* life stages of ~1-10 μm in diameter within an area of approximate diameter ≤175 μm, with life stages distinguished from background fluorescent artifacts on the basis of fluorescence color and intensity. One infectious focus was taken to correspond to a single infectious oocyst. A composite image assembled by splicing together images of all 1 mm² sections for a single well analyzed in this manner is shown in Figure S1a. Infectious foci are visible as distinct fluorescent “points”. An example of a single infectious focus at 100× magnification is shown in Figure S1b.

Text S3. Simulated and Natural Solar Irradiation Procedures

Simulated sunlight experiments. Experimental sets 1 and 4 (see Table S2) were undertaken in 50-mL crystallization dishes in duplicate, with thermostating at 25 °C, according to the procedures described in Forsyth et al. (2013).² Experimental set 3 (Table S2) was undertaken according to the same general procedures as for sets 1 and 4, but using N₂-sparged solutions in a 300-mL gas-tight reactor, also as described in Forsyth et al. (2013).² Samples were irradiated using a Model 66924 arc lamp source equipped with a 450-W O₃-free Xe arc lamp, focusing collimator, atmospheric attenuation filter (cutoff of $\lambda < 290$ nm), and dichroic mirror (Newport-Oriel). The FAC only and FAC + light experiments for each set were undertaken at [FAC]₀ = 8 mg L⁻¹ as Cl₂. In some cases, FAC was redosed to 8 mg L⁻¹ as Cl₂ after a certain irradiation time to permit continuation of experiments after depletion of the initially dosed FAC.

Natural sunlight experiment. Natural sunlight experiments (designated as experimental set 2 in Table S2) were undertaken in duplicate 30-mL quartz test tubes at ambient temperature (34 ± 2 °C), according to the general procedures described in Forsyth et al. (2013).² Samples were irradiated by placing them on the roof of the More Hall Civil and Environmental Engineering building under clear skies between 2:00 and 3:00 PM on 7/10/14. Temperature was monitored by means of a thermometer in a paired control containing the same experimental matrix as treated samples, absent oocysts and FAC. Sample tubes were inclined at an angle of 30° from the horizontal (roughly equivalent to the solar zenith angle in Seattle, WA, at mid-afternoon on 7/10/14), and reaction solutions were continuously stirred using PTFE-coated magnetic stir bars and a multi-position magnetic stir plate. Dark control (FAC only) experiments were undertaken in the same manner as for simulated sunlight experiments, but with thermostating at 34 °C. FAC only and FAC + light experiments were undertaken at initial [FAC] levels of 8 mg L⁻¹ as Cl₂. FAC was redosed to 8 mg L⁻¹ as Cl₂ after 30 minutes of irradiation in order to permit continuation of experiments after depletion of the initially dosed FAC.

Text S4. Spectroradiometric and Actinometric Measurements

Spectral irradiance measurements were obtained using a USB2000+ XR spectroradiometer (Ocean Optics) equipped with a 200 µm × 2 m optical fiber and a CC-3-UV-S cosine corrector. Incident irradiance spectra were obtained for each light source with the cosine corrector aligned perpendicular to the plane of the water sample being irradiated, at the elevation of the water surface relative to the light source, and directly toward the light source. Overall incident irradiances, W (in W m⁻²), were obtained from 290 to 400 nm by integration of the area under the resulting spectral irradiance curves, yielding representative values of $W_{SS, \lambda=290-400nm} =$

82 W m⁻² and 112 W m⁻² for simulated sunlight in 50-mL crystallization dishes and the 300-mL reactor used for anoxic experiments, respectively, and $W_{NS,\lambda=290-400nm} = 38 \text{ W m}^{-2}$ for natural sunlight in quartz tubes (compared to 46 W m⁻² over the same wavelength range for the ASTM G173-03 standard for solar radiation – hemispherical on a 37° tilted surface – at sea level³). Representative incident spectral irradiance curves are depicted for simulated and natural sunlight, in comparison to the ASTM G173-03 standard at sea level, in Figure S2.³

Effective in situ fluence rates, $F_{tot,\lambda=290-400nm}$, from 290-400 nm were determined by means of *p*-nitroanisole (PNA)/pyridine actinometry for simulated sunlight and natural sunlight experiments.⁴ Actinometer solutions containing 1 μM PNA and 10 mM pyridine were prepared in Milli-Q water. These actinometer solutions were then transferred into the same 50-mL crystallization dishes or 300-mL reactor as used for disinfection experiments under simulated sunlight, or the same 30-mL quartz tubes as used for disinfection under natural sunlight. The actinometer solutions were kept in the dark until the start of each experiment, after which they were exposed to light for similar durations as utilized in the oocyst inactivation systems. Samples were obtained from the irradiated actinometer solutions at pre-defined intervals for PNA analysis. PNA concentrations were measured on an UltiMate 3000 HPLC-UV system (Thermo Scientific/Dionex), using isocratic elution on a Supelco Ascentis C18 column (150 × 2.1 mm, 3 μm), with 50:50 CH₃CN:10-mM H₃PO₄ as mobile phase. Values of $F_{tot,\lambda=290-400nm}$ (in units of J m⁻² s⁻¹, or W m⁻²) were determined from PNA loss rates in accord with established procedures.^{5,6}

Text S5. Competition kinetics measurements.

The value of k_5 (for reaction of O(³P) with *t*BuOH) was determined by means of competition kinetics,⁷ using an approach in which the initial rate of O₃ production from reaction

of O(³P) with constant [O₂] was monitored in the presence of varying [*t*BuOH]. O(³P) was generated through photolysis of [FAC]₀ = 8 mg L⁻¹ as Cl₂ under simulated sunlight in pH 8.0, 10-mM phosphate buffer at 25 °C, using the same reactor setup as for experimental sets 1 and 4 above. Experiments were undertaken in the presence of [O₂] = 2.8 × 10⁻⁴ M and [*t*BuOH] = 0–2.5 × 10⁻¹ M, as well as 2.5 × 10⁻⁶ M of an O₃ probe compound, cinnamic acid, which reacts rapidly (*k* = 3.8 × 10⁵ M⁻¹s⁻¹ at pH 8) and selectively with O₃ to yield 1 mol benzaldehyde/mol O₃ consumed.⁸ Under these conditions, the cinnamic acid concentration is high enough to trap ~100% of O₃ generated at early times (<90s) without disturbing O(³P) levels. Initial rates of O₃ formation were determined in such solutions by monitoring buildup of benzaldehyde from 0-60 seconds after initiation of FAC photolysis. Benzaldehyde concentrations were measured with an UltiMate 3000 HPLC-UV system (Dionex), using gradient elution on an Ascentis RP Amide column (150 × 2.1 mm, 3 μm), with CH₃CN and 10-mM H₃PO₄ as mobile phases.

The data from these experiments were evaluated according to eq S1,⁷

$$\frac{(\Delta[\text{O}_3]/\Delta t)_0}{(\Delta[\text{O}_3]/\Delta t)} - 1 = \frac{(\Delta[\text{O}_3])_0}{(\Delta[\text{O}_3])} - 1 = \frac{k_5[\text{tBuOH}]}{k_3[\text{O}_2]} \quad (\text{S1})$$

where (Δ[O₃]/Δ*t*)₀ is the initial O₃ formation rate in the absence of *t*BuOH (for Δ*t* = 60 s), (Δ[O₃]/Δ*t*) the initial O₃ formation rate at a given value of [*t*BuOH], *k*₅ the second-order rate constant for reaction of O(³P) with *t*BuOH, and *k*₃ the second-order rate constant (4.0 × 10⁹ M⁻¹s⁻¹)⁹ for reaction of O(³P) with O₂. The value of *k*₅ was in turn obtained from the slope of a plot of

$\frac{(\Delta[\text{O}_3]/\Delta t)_0}{(\Delta[\text{O}_3]/\Delta t)} - 1$ versus $\frac{[\text{tBuOH}]}{[\text{O}_2]}$, as shown in Figure S4.

139 **Table S1.** Characteristics of Tolt River WTP sample.

Parameter	Value
pH	8.0 ^a
DOC (mg C L ⁻¹)	1.2
Carbonate alkalinity (mg L ⁻¹ as CaCO ₃)	9.5
SUVA ₂₅₄ (L mg ⁻¹ m ⁻¹)	3.0
SUVA ₃₁₃ (L mg ⁻¹ m ⁻¹)	1.2
SUVA ₃₆₅ (L mg ⁻¹ m ⁻¹)	0.4

140 ^a Sample buffered at pH 8.0 using 10-mM phosphate (native pH = 7.0)

141
142
143 **Table S2.** General experimental conditions and corresponding *C. parvum* oocyst stock information

Experimental Set	Conditions ^a	Lot #	Shedding Dates	Purification Date	Receipt Date	Disinfection Date	Days from Shedding to Disinfection
1	pH 8.0 PB, 25 °C, SS	140325	3/21/14-3/25/14	3/25/2014	3/26/2014	4/3/2014	9
2	pH 8.0 Tolt water, 34(±2) °C, NS	140613	6/9/14-6/13/14	6/13/2014	6/17/2014	7/10/2014 ^b	27 ^b
3	pH 8.0 PB, 25 °C w/o O ₂ , SS	140410	4/7/14-4/10/14	4/10/2014	5/28/2014	6/5/2014	56
4	pH 8.0 PB, 25 °C w/ <i>t</i> BuOH, SS	140410	4/7/14-4/10/14	4/10/2014	5/28/2014	5/29/2014	49

144 ^a PB – 10-mM phosphate buffer, SS – simulated sunlight, NS – natural sunlight; ^b The accompanying FAC only experiment for this set
145 was undertaken on 7/17/14 (i.e., oocysts in the FAC only experiment were 34 days old).

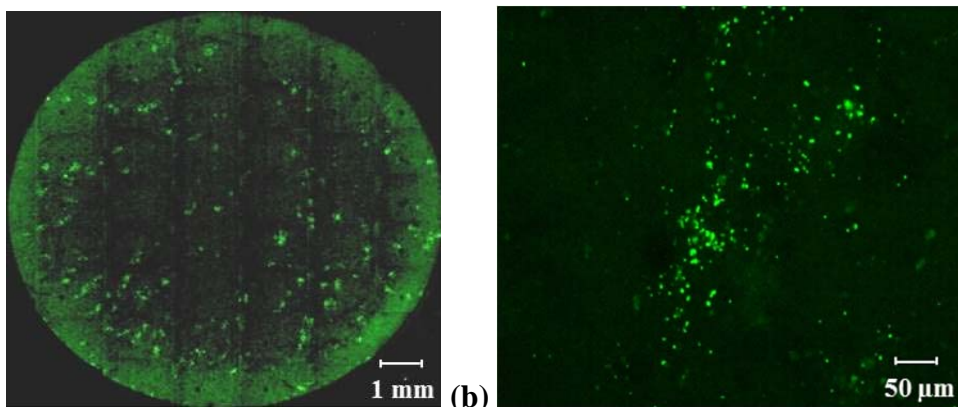


Figure S1. Examples of (a) a typical well in a 48-well plate, and (b) a single infectious focus within such a well, as analyzed by the CC-IFA method. Images (a) and (b) were obtained using an inverted epifluorescence microscope with 10× objective at 40× magnification* and 100× magnification, respectively. *Image (a) is a composite of multiple images taken at 40× magnification for each 1 mm² section of a grid spanning the entirety of the well, with all 1 mm² images spliced together by the MetaMorph[®] software used for counting. Infectious foci (defined as clusters of *Cryptosporidium* intracellular developmental stages originating from infection by a single oocyst) are visible as distinct fluorescent “points” in image (a).

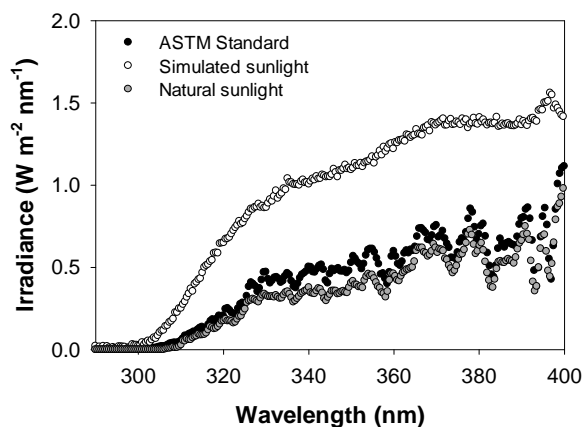


Figure S2. Direct incident spectral irradiance curves between 290 and 400 nm for (i) the Newport Solar Simulator (with dichroic mirror and atmospheric attenuation filter) at beam center and the surface of irradiated reactor solutions, and (ii) natural sunlight on the roof of More Hall (Seattle, WA) at 2:00PM on 7/10/14, at an angle of 30° from the horizontal, compared to the ASTM G173-03 solar irradiance standard (hemispherical on a 37° tilted surface). Spectroradiometric measurements were taken using an Ocean Optics USB2000+ XR spectroradiometer equipped with a 200 μm × 2 m optical fiber and a CC-3-UV-S cosine corrector.

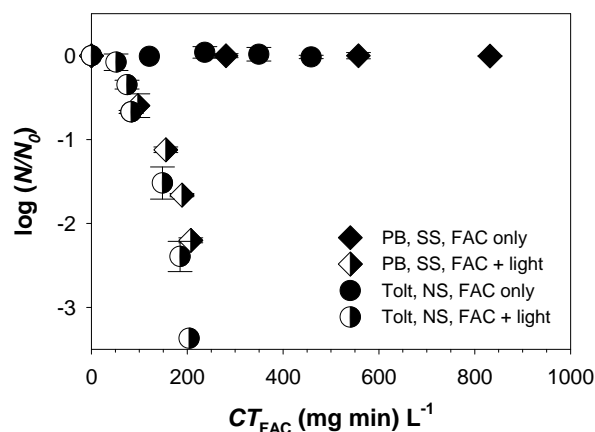


Figure S3. Residual infectivity of *C. parvum* Iowa strain (Harley Moon) oocysts versus CT_{FAC} levels reached during exposure of FAC-containing pH 8.0, 10-mM phosphate buffer (PB) to simulated sunlight (SS) at 25 °C, and during exposure of FAC-containing pH 8.0 Tolt River WTP water (Tolt) to natural sunlight (NS) at ambient temperature (34 ± 2 °C), compared to corresponding FAC only controls. See Table S2 (experimental sets 1 and 2) for details on the oocyst stocks used in each experiment.

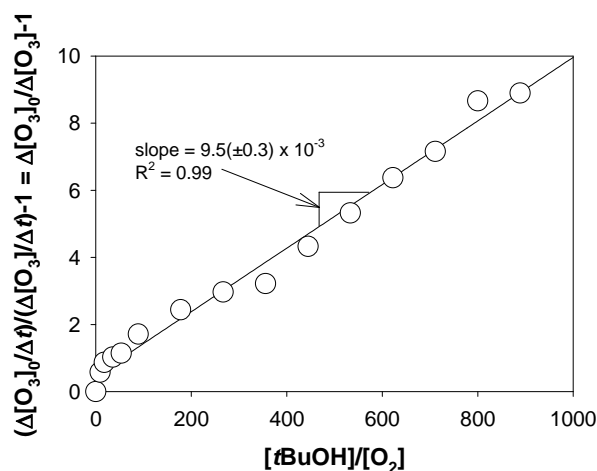
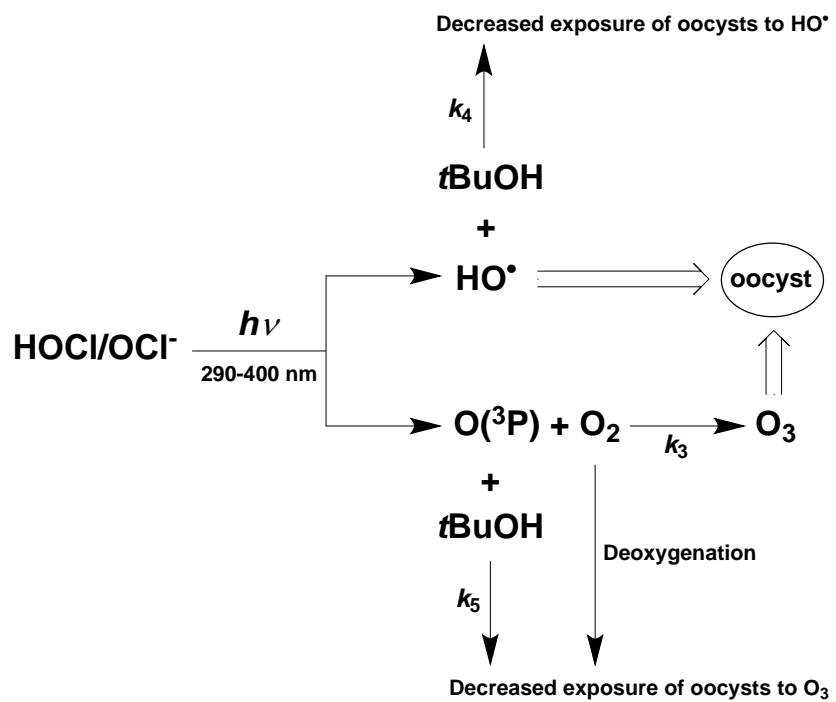


Figure S4. Competition kinetics plot obtained from measurements of the initial rate of O_3 formation in the reaction of 2.8×10^{-4} M O_2 with $O(^3P)$ in the presence of varying concentrations of *t*BuOH (0 – 2.5×10^{-1} M). $O(^3P)$ was generated through the simulated sunlight-driven photolysis of $[FAC]_0 = 8$ mg L^{-1} as Cl_2 in pH 8.0, 10-mM phosphate buffer at 25 °C. Initial O_3 formation rates were determined over the first 60 seconds of photolysis, based on the buildup of benzaldehyde in the presence of 2.5×10^{-6} M cinnamic acid.



Scheme S1. Effects of deoxygenation and *t*BuOH amendment on oocyst inactivation during FAC photolysis.

Literature Cited

- (1) Johnson, A. M.; Di Giovanni, G. D.; Rochelle, P. A., Comparison of assays for sensitive and reproducible detection of cell culture-infectious *Cryptosporidium parvum* and *Cryptosporidium hominis* in drinking water. *Appl. Environ. Microbiol.* **2012**, 78, 156-162.
- (2) Forsyth, J. E.; Zhou, P.; Mao, Q.; Asato, S. S.; Meschke, J. S.; Dodd, M. C., Enhanced inactivation of *Bacillus subtilis* spores during solar photolysis of free available chlorine. *Environ. Sci. Technol.* **2013**, 47, 12976-12984.
- (3) *Standard G173 – 03 (Reapproved 2008): Standard Tables for Reference Solar Spectral Irradiances: Direct Normal and Hemispherical on 37° Tilted Surface*, ASTM: Philadelphia, PA, 2012
- (4) Dulin, D.; Mill, T., Development and evaluation of sunlight actinometers. *Environ. Sci. Technol.* **1982**, 16, 815-820.
- (5) Schwarzenbach, R. P.; Gschwend, P. M.; Imboden, D. M. *Environmental Organic Chemistry*; 2nd ed.; John Wiley & Sons, Inc.: Hoboken, NJ, 2003.
- (6) Zepp, R. G., Quantum yields for reaction of pollutants in dilute aqueous solution. *Environ. Sci. Technol.* **1978**, 12, 327-329.
- (7) Muñoz, F.; von Sonntag, C., Determination of fast ozone reactions in aqueous solution by competition kinetics. *J. Chem. Soc. Perk. Trans. 2* **2000**, 2, 661-664.
- (8) Leitzke, A.; Reisz, E.; Flyunt, R.; von Sonntag, C., The reactions of ozone with cinnamic acids: formation and decay of 2-hydroperoxy-2-hydroxyacetic acid. *J. Chem. Soc., Perk. Trans. 2* **2001**, 793-797.
- (9) Klaening, U. K.; Sehested, K.; Wolff, T., Ozone formation in laser flash photolysis of oxoacids and oxoanions of chlorine and bromine. *J. Chem. Soc., Faraday Trans. 1* **1984**, 80, 2969-2979.